Nucleic Acids Research, 2004, Vol. 32, No. 16 ***4915–4924***
doi:10.1093/nar/gkh837

Conserved tertiary base pairing ensures proper RNA folding and efficient assembly of the signal recognition particle *Alu* domain

Laurent Huck, Anne Scherrer, Lionel Terzi, Arthur E. Johnson[1], Harris D. Bernstein[2], Stephen Cusack[3], Oliver Weichenrieder[3] and Katharina Strub*

Département de Biologie Cellulaire, Université de Genève, CH-1211 Genève 4, Switzerland, [1]Department of Medical Biochemistry and Genetics, Texas A&M University, System Health Science Center, College Station, TX 77843-1114, USA, [2]Genetics and Biochemistry Branch, National Institute of Diabetes and Digestive and Kidney Diseases, National Institute of Health 10, Center Drive, Bethesda, MD 20892-1810, USA and [3]European Molecular Biology Laboratory, Grenoble Outstation, 6, Rue Jules Horowitz, F-38042 Grenoble, CEDEX 9, France

Received July 29, 2004; Revised and Accepted September 2, 2004

ABSTRACT

Proper folding of the RNA is an essential step in the assembly of functional ribonucleoprotein complexes. We examined the role of conserved base pairs formed between two distant loops in the *Alu* portion of the mammalian signal recognition particle RNA (SRP RNA) in SRP assembly and functions. Mutations disrupting base pairing interfere with folding of the *Alu* portion of the SRP RNA as monitored by probing the RNA structure and the binding of the protein SRP9/14. Complementary mutations rescue the defect establishing a role of the tertiary loop–loop interaction in RNA folding. The same mutations in the *Alu* domain have no major effect on binding of proteins to the S domain suggesting that the S domain can fold independently. Once assembled into a complete SRP, even particles that contain mutant RNA are active in arresting nascent chain elongation and translocation into microsomes, and, therefore, tertiary base pairing does not appear to be essential for these activities. Our results suggest a model in which the loop–loop interaction and binding of the protein SRP9/14 play an important role in the early steps of SRP RNA folding and assembly.

INTRODUCTION

The assembly of ribonucleoprotein particles (RNPs) is a complex process that includes multiple steps such as proper folding of the RNA moiety and the ordered concomitant or sequential association of the proteins at specific subcellular locations. Folding of RNAs with sizes ⩾300 nt is rather slow and may be assisted by proteins with RNA chaperone activities and by specific RNA binding proteins, which may remain part of the RNP. Reasons for the slow folding of RNA molecules include their highly complex tertiary structure as well as their intrinsic propensity to become kinetically trapped in inactive structures [for review see (1,2) and references therein].

The goal of this study was to examine the specific role of an RNA tertiary structure in the *Alu* domain of the mammalian signal recognition particle (SRP). SRP is probably one of the best-characterized ribonucleoprotein complexes, since it can be assembled and studied *in vitro*. SRP plays an essential role in targeting proteins to the endoplasmic reticulum (ER) [for review see (3)], which is the first step in routing proteins into the secretory pathway. SRP specifically recognizes signal sequences, a common hallmark of ER-targeted proteins, in nascent polypeptide chains as they exit from the ribosome and subsequently delays elongation of the nascent chain. SRP then targets the ribosome-nascent chain complex to the translocon, a specific structure in the ER membrane that promotes the transfer of the nascent chain across or into the ER membrane [for review see (4)].

SRP has a two-domain structure in most but not all organisms [for review see (5)]. The S domain of mammalian SRP comprises the central part of SRP RNA (or 7SL RNA) and the proteins SRP68/72, SRP54 and SRP19 (Figure 1). The conserved RNA helix VIII and SRP54 harbour the signal recognition and the targeting functions of SRP (6,7). The *Alu* domain, which comprises the 5′ and 3′ ends of SRP RNA and the protein SRP9/14, retards or arrests the elongation of the nascent chain and thereby increases the translocation efficiency *in vitro* (6,8,9). Over the last few years, a vast body of atomic structure information was obtained [for review see (10–12)] and the positioning of SRP on the ribosome was reconstructed from cryo-electron microscopy (cryo-EM) images (13). This information has yielded new insights into the mechanism of SRP functions and has facilitated a more specific biochemical analysis.

SRP is thought to assemble in nucleoli, because SRP RNA and SRP proteins, except SRP54, can be observed in this

*To whom correspondence should be addressed. Tel: +41 22 379 6724; Fax: +41 22 379 6442; Email: Strub@cellbio.unige.ch
Present address:
Oliver Weichenrieder, Dept. of Molecular Carcinogenesis—H2, The Netherlands Cancer Institute, Plesmanlaan 121, 1066 CX Amsterdam, Netherlands

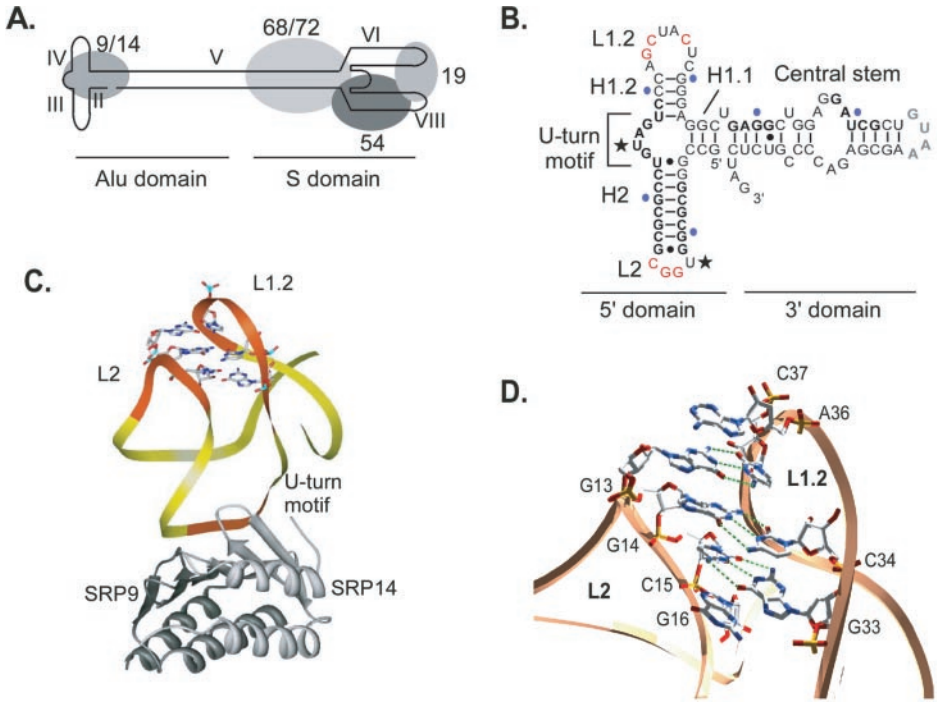

Figure 1. Structure of SRP and the SRP *Alu* domain. (**A**) Schematic representation of SRP, (**B**) secondary structure of the minimal *Alu* RNA that still binds 9/14 efficiently. Stems and loops are named according to the topological nomenclature. Bases in the loops that form tertiary base pairs are highlighted in red. Protein footprints are shown in boldface. U-turns are marked with asterisks and stretches of 10 nt are marked in blue. The U-turn motif marks a highly conserved sequence that represents the major protein-binding site. (**C**) Structure of the SRP *Alu* 5′ domain. SRP9 and SRP14 are displayed as dark and light grey ribbons, respectively. The RNA is shown as a yellow ribbon with the loop sequences and the U-turn motif shown in orange. Nucleotides from loops L2 and L1.2 that are involved in tertiary interactions between the loops are shown as wireframe. (**D**) Detailed view of the tertiary base pairing between loops. Bases G13, G14 and C15 form hydrogen bonds with C37, C34 and G33, respectively (dotted green lines). One base from each loop, G16 and A36, are positioned to extend the stack formed by the three base pairs.

structure (14–16). The localization of SRP RNA to the nucleolus is dependent on the *Alu* sequences and on the RNA helix VIII (17). In addition, import of SRP proteins into nucleoli and export of SRP RNA are mediated by specific receptors (18–20). Till date, nothing is known about the specific events that couple RNA synthesis and folding to the ordered assembly of SRP proteins.

An *Alu* domain-like structure is present in all eukaryotic and archaeal and in few eubacterial SRP RNAs. The common signature of this domain is a three-way junction of stems and a highly conserved single-stranded region (21,22). Of the SRP RNAs including an *Alu* domain, the yeast and protozoan RNAs are missing one or both hairpins. In trypanosomes, the absence of one hairpin in the *Alu* domain may have been compensated for by the acquisition of an additional transfer RNA (tRNA)-like RNA in the SRP particle (23,24).

As revealed by crystallography, the *Alu* domain contains a compactly folded three-way junction of stems. A stack of two stems (H1.1 and H1.2) and a third stem (H2) are connected by a single-stranded U-turn at this junction [Figure 1; (25)]. Note that we use the topological nomenclature in which helix H2 and loop L2 represent stem–loop III and helix H1.2 and loop L1.2 stem–loop IV in the helix diagram of Figure 1A [according to the nomenclature in (26)]. The single-stranded connecting region is highly conserved in primary sequence and represents the major protein-binding site [Figure 1B, U-turn motif; (22,25)]. The U-turn determines the relative orientation of the two helical stems. The RNA fold is further stabilized by a tertiary structure consisting of three G-C base pairs, which are formed between the two distant loops L1.2 and L2 (Figure 1D, G13-C37, G14-C34 and C15-G33). The three base pairs form an extended stack together with two purines from the loops L2 and L1.2 (G16 and A36). The existence of loop–loop interactions had previously been suggested based on sequence complementarities observed between the two loops (27).

The protein SRP9/14 also makes contacts to the central stem connecting the *Alu* and the S domains (Figure 1B). Further biochemical and structural data support a model in which the central stem would fold back by up to 180° to align alongside the 5′ domain allowing contacts to the SRP9 moiety of the protein (25,28). The model is consistent with the requirement that the 3′ and the 5′ domains have to be flexibly linked for fully efficient binding of SRP9/14 (29).

After the existence of loop–loop interactions had been confirmed and their identity revealed by crystal structure, we decided to examine their role in SRP assembly and function. Base pairs were disrupted by specific individual mutations in both loops and restored with a different primary sequence by simultaneous complementary mutations. The mutated RNAs were analysed by native gel electrophoresis and by limited V1 ribonuclease digestion experiments and assayed for SRP9/14 binding. The mutated SRP RNAs were also reconstituted into SRP and their activities compared to the activities of SRP comprising wild-type (WT) RNA. Our results demonstrate that base pairing between the loops is

important for proper folding of the SRP RNA *Alu* domain. The mutations in the *Alu* domain had no significant impact on the binding of the S domain proteins, suggesting that it can fold independently. Despite the folding defects, all but one mutant RNA could be assembled into SRPs with intact elongation arrest and translocation activities, indicating that base pairing is not essential for these activities.

MATERIALS AND METHODS

Materials

Sources of materials were as follows: urea, AppliChem; 4-(2-hydroxyethyl)-1-piperazine-1-ethane sulfonic acid (HEPES), AppliChem; potassium and magnesium acetate [KOAc and $Mg(OAc)_2$], Fluka; Nikkol–BL-85Y, Nikko Chemical Co.; Triton X-100, Interchim; [^{35}S]methionine (1500 μCi/mmol), Amersham Biosciences; Aquaphenol, QbioGene; DTT, Eurobio; spermidine, Tris[hydroxymethyl] aminomethane (Tris), BSA and ribonucleotides, Sigma. The T7 RNA polymerase expression plasmid was a kind gift of Dr Mallet (30). The T7 RNA polymerase was kindly prepared by Viviane Simonet, Julien Hasler and L. Terzi.

Mutation and expression of the SRP RNA gene

Mutations at specific sites in the SRP RNA gene were introduced by PCR using the QuickChange™ method (Stratagene). The primer oligonucleotides contained the desired mutations flanked by 15 nt (Microsynth). The template for PCR was the plasmid p7Sswt (22). Two sequential rounds of mutations yielded the clones with complementary mutations. All clones were verified by automatic sequencing. Plasmids were linearized with XbaI (Gibco BRL) before synthesis of the RNA with T7 RNA polymerase in 100 μl reactions containing 40 mM Tris-HCl, pH 8.1, 7 mM $MgCl_2$, 1 mM spermidine, 5 mM DTT, 1 mM of each rNTPs, 1 μg/μl BSA, 100 ng/μl DNA template and 0.1μg /μl T7 RNA polymerase. After transcription, the DNA was digested with RQ1 RNAse-free DNAse (Promega) and the samples extracted with phenol and purified on 1 ml Sephadex G50 (fine, Pharmacia) or on Nucleobond (Machery & Nagel) columns. The RNAs were precipitated and dissolved in sterile water. To optimize protein binding with biotinylated SRP RNAs, we tested different ratios of UTP/bio-11-UTP (ENZO Life Sciences) in the transcription reactions. Protein binding was optimal when using equal ratios of both nucleotides. RNA concentrations were determined by OD_{260} and the quality of the RNA samples analysed by denaturing 6% PAGE. The concentrations of biotinylated RNAs were determined by comparing three dilutions of each sample to a dilution series of an RNA standard of unmodified WT RNA with ethidium-bromide-stained denaturing PAGE. Canine SRP RNA was extracted from the DEAE resin used to disassemble SRP into RNA and protein subunits (6).

RNA analysis

Native gels (acrylamide–bisacryamide ratio of 40:1) were run in 50 mM Tris, pH 7.5 and 10 mM $Mg(OAc)_2$ in the cold room at 0.22 W/cm^3 for 4 h. The samples were loaded in 20 mM KOAc and 3 mM $Mg(OAc)_2$ neutralized to pH 7.5 and 40% glycerol. Native RNA was stained with GelStar® (Cambrex). One microgram of RNA was digested with V1 RNAse (Pierce, 0.05 U per reaction) in 20 μl of 300 mM KOAc, 3 mM $Mg(OAc)_2$ and 10 mM HEPES, pH 7.5 for 20 min on ice. The reactions were stopped and the RNAs purified with phenol/dichloromethane extractions. The precipitated RNA was dissolved in formamide loading buffer and displayed by 10% PAGE. The RNA was revealed by ethidium bromide staining of the gel and visualized on an ultraviolet light box.

RNA binding assays

Synthetic mRNAs for human SRP14, human SRP19 and canine SRP54 were prepared as described previously in (31–33), respectively. The [^{35}S]methionine-labelled h14 was synthesized in wheat germ translation reactions in the presence of 3 pmol of recombinant h9 (34) and 6 pmol of recombinant h9/14 in 10 μl translation reaction. For the binding reactions, an aliquot of 3.3 μl was combined with the desired amounts of biotinylated RNA in a final volume of 50 μl of binding buffer (50 mM HEPES–KOH, pH 7.5, 500 mM KOAc, pH 7.5, 5 mM $Mg(OAc)_2$ and 0.01% Nikkol). The complex was allowed to form for 10 min on ice and then for 10 min at 37°C. The magnetic streptavidin beads (Dynabeads M-280, Dynal Biotech ASA) were prepared as indicated by the manufacturer and equilibrated with binding buffer. The beads (60 μl) were combined with the protein–RNA samples and incubated for another hour at 4°C. The bound samples were washed three times for 10 min with binding buffer including 0.1% Triton X-100. Bound proteins were analysed by 15% SDS–PAGE, visualized by autoradiography and quantified with the PhosphoImager (Bio-Rad). We confirmed by denaturing PAGE and ethidium bromide staining that no detectable amounts of SRP RNA were present in the unbound fractions at the highest RNA concentrations used (detection limit 25 ng). In addition, the protein contents of the supernatant fractions were also quantified in the initial experiments. The bound and free proteins together accounted for the total protein input (100 ± 10%) confirming that dissociation of the complex was negligible during the wash. A negative control RNA, rat 4.5S RNA (34), showed no detectable protein-binding activity (data not shown). For the binding reactions with h19 and c54, the translation reactions contained 6 pmol of recombinant h19 and 6 pmol of recombinant h19 and c54, respectively.

SRP proteins

The proteins h9, h14 and h19 were expressed in *Escherichia coli* from the plasmid pEh9, pEh14 and pE19 (8,34) using the T7 RNA polymerase expression system (35). Cells were lysed in a French Press™ and the extracts of h9 and h14 were combined for the purification of the complex. Hi-Trap Heparin (Amersham Biosciences), hydroxyl apatite (Bio-Rad) and Superdex-200 (Amersham Biosciences) chromatography was used to purify h9/14. Hi-Trap Heparin, CM and Superdex-200 (Amersham Biosciences) chromatography was used to purify hϕ19. c54 was expressed in insect cells using the baculovirus expression system (7). Following lyses of the cells in the homogenizer, the protein was purified by CM and Hi-Trap Heparin chromatography. The purified proteins were quantified by spectrophotometry at 280 nm. Molar extinction coefficient $\varepsilon_{h9/14}$, 15 130 M^{-1} cm^{-1}; ε_{h19}, 12 570 M^{-1} cm^{-1}; and ε_{54},

22 220 M^{-1} cm^{-1}. Canine SRP68/72 was purified from canine SRP as described previously (6). SRP68/72 was quantified by comparing the SRP68 signal to known concentrations of BSA in a Coomassie-stained SDS–PAGE.

Particle reconstitutions and activity assays

Particles were reconstituted as described previously (36) in 50 µl reactions at 2 µM protein concentrations and 4 µM RNA concentrations for WT and 2Comp RNAs. 2L2 and 3L2 RNAs were used at final concentrations of 16 and 24 µM, respectively. Fifty microliters DEAE Sephacel (Pharmacia) columns were eluted twice with 50 µl of 20 mM HEPES–KOH, pH 7.5, 500 mM KOAc, pH 7.5, 5 mM $Mg(OAc)_2$, 0.01% Nikkol and 1 mM DTT. Active SRP is eluted in the first fraction. In the reactions with 2L2 and 3L2 RNAs, we first eluted with 30 µl followed by two fractions of 50 µl to optimize the yield of active SRP. One-tenth of the total fraction was analysed by 5–20% SDS–PAGE and visualized by silver staining. c54 samples containing 50, 100, 150 and 200 ng of protein were run on the same gel and used to estimate the particle concentrations. For the direct assays, reconstitutions were done in 8 µl at 0.5 and 1 µM final concentrations of canine SRP68/72, recombinant h9/14, h19 and c54 and *in vitro* synthesized SRP RNAs, respectively. Activity assays were done as described previously (8) at final particle and membrane concentrations of 100 nM and 0.15 eq/µl, respectively. Preprolactin, prolactin and cyclin D were quantified by the use of a phosphorescence imaging system (Bio-Rad). Elongation arrest and translocation efficiencies were calculated as follows:

$$EA = \left(1 - \frac{Ps/Cs}{Po/Co}\right) \times 100,$$

where EA is the percentage elongation arrest activity, Ps and Cs are the amounts of preprolactin and cyclin quantified in the sample and Po and Co the amounts of preprolactin and cyclin present in the negative control (SRP buffer or SRP reconstituted without h9/14). $T = 100 \times [P/(pP + P)]$, where T is the percentage translocation, P is the amount of prolactin and pP the amount of preprolactin quantified in each sample. All SRPs were tested in at least two independent experiments.

Computer programs and data bases

For the sequence comparison of SRP RNAs, we used the SRP database (21). Molecular graphics images were produced using the UCSF Chimera package from the Computer Graphics Laboratory, University of California, San Francisco (supported by NIH P41 RR-01081) and the Swiss PDB viewer using Pov-Ray™ (http://www.expasy.org/spdbv/).

RESULTS

Tertiary base pairing and structural determinants in loop L2 are conserved in evolution

To examine the conservation of structural determinants in the loops L1.2 and L2, we created a new structure-based alignment of the loop sequences. In mammalian SRP RNA, loop L2 is well defined by the sheared G-G base pair and has a rather stiff character determined by another U-turn (U12, Figure 1B, asterisk). In contrast, loop L1.2 lacks internal stabilizing elements and is, therefore, presumed to be flexible. Its most important structural feature is its capacity to form base pairs with loop L2 (25). For the analysis, we included SRP RNAs [SRPDB; (21)] containing the three-way junction of stems forming the specific fold of the mammalian SRP *Alu* domain (Figure 2). As illustrated by the helix diagrams, the lengths of the stems and the sizes of the loops are remarkably different.

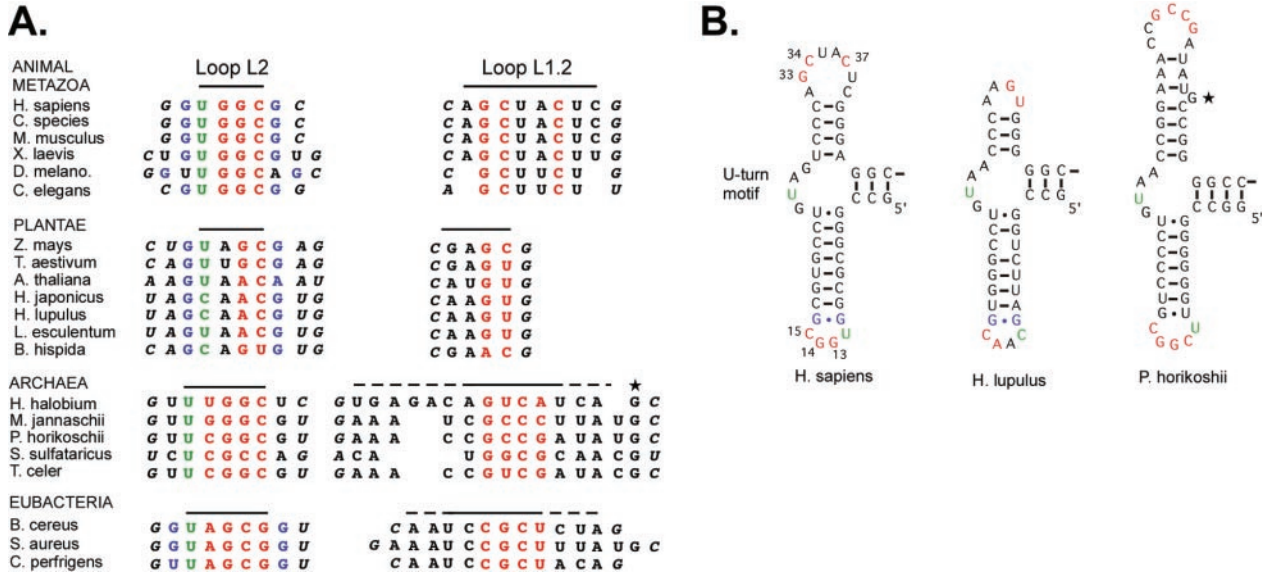

Figure 2. Structure-based alignment of loop L1.2 and L2 sequences in SRP RNAs of animal metazoans, of plants and of eubacterial and archaeal species. (**A**) Nucleotides proposed to base pair are shown in red, sheared G-G pairs in blue and U-turns in green. First nucleotides in stems are shown in italic. Black bars delineate the loop sequences. For each species, only one representative is shown. Sequences were obtained from SRPDB. (**B**) Helix diagrams of mammalian, plant and archaeal *Alu* RNA 5′ domains. Asterisks highlight a conserved nucleotide in the archaeal RNAs. The helix diagram of a eubacterial SRP RNA resembles most closely the one of archaeal SRP RNAs.

The G-G base pair and the adjacent U-turn are well conserved in loop L2 of all but archaeal SRP RNAs (Figure 2, blue and green). In these organisms, the boundaries of the loop L2 are well defined by these structural elements. Since the G-G base pair is absent in archaeal RNAs, the boundaries of loop L2 remain uncertain and the putative U-turn motif may, therefore, precede the one shown. In a few species, the uridine is replaced by a cytidine, which may also introduce U-turn-like bends as revealed by the pseudoknot structure of beet western yellow virus RNA (37). In four A*rabidopsis* species, the G-G base pair is replaced by a G-A base pair.

The potential to form base pairs is conserved in all SRP RNAs with a remarkable bias for G-C pairs (Figure 2, red nucleotides). More strikingly, in animal metazoans even the primary sequences of the nucleotides are conserved. In plants, only 2 bp may form between the loops because of the smaller size of loop L1.2. In contrast, in Archaea and Eubacteria the increased size of loop L2 expands the predicted base complementarities between the loops. In these organisms, helix H1.2 is not well defined, since the loop-adjacent strands are purine-rich on both sides and it remains uncertain to which degree they may form non-canonical base pairs to extend the four Watson–Crick base pairs.

In summary, the high conservation of loop–loop base pairing and of structural determinants in loop L2 points towards a role of these structures in SRP assembly and function. However, apart from base pairing, the shape and size of the tertiary structure is expected to vary considerably, since the number of base pairs and the sizes of the loops are not conserved between different RNAs.

Mutations in loop L2 induce conformational changes in the RNA *Alu* domain

To examine the functions of the tertiary base pairs in human SRP RNA, we changed bases in single loops to disrupt base pairing and in both loops to restore base pairing with a different sequence (see Table 1). Guanidine was replaced by cytidine and vice versa. The RNAs were synthesized *in vitro*. They were never denatured and were purified under native conditions to avoid refolding artefacts. The mutated and wild-type synthetic RNAs migrated as a single band at the position expected of their size in denaturing gel electrophoresis (Figure 3A, lower panel).

To examine the conformation of the synthetic RNA variants, they were displayed in parallel with native canine SRP RNA by native PAGE (Figure 3A). Native canine SRP RNA migrated as a single band. *In vitro* synthesized RNAs are more heterogeneous, containing RNA aggregates and RNAs with

Table 1. Mutations in SRP RNA

Wild type		
WT	Loop L2	5′-G13 — G14-C15-3′
	Loop L1.2	3′-C37-(A36-U35)-C34-G33-5′
Mutations in a single loop		
2L2	Loop L2	5′-C13 — C14-C15-3′
	Loop L1.2	3′-C37-(A36-U35)-C34-G33-5′
3L2	Loop L2	5′-C13 — C14-G15-3′
	Loop L1.2	3′-C37-(A36-U35)-C34-G33-5′
2L1.2	Loop L2	5′-G13 — G14-C15-3′
	Loop L1.2	3′-G37-(A36-U35)-G34-G33-5′
3L1.2	Loop L2	5′-G13 — G14-C15-3′
	Loop L1.2	3′-G37-(A36-U35)-G34-C33-5′
Compensatory mutations in both loops		
2Comp	Loop L2	5′-C13 — C14-C15-3′
	Loop L1.2	3′-G37-(A36-U35)-G34-G33-5′
3Comp	Loop L2	5′-C13 — C14-G15-3′
	Loop L1.2	3′-G37-(A36-U35)-G34-C33-5′

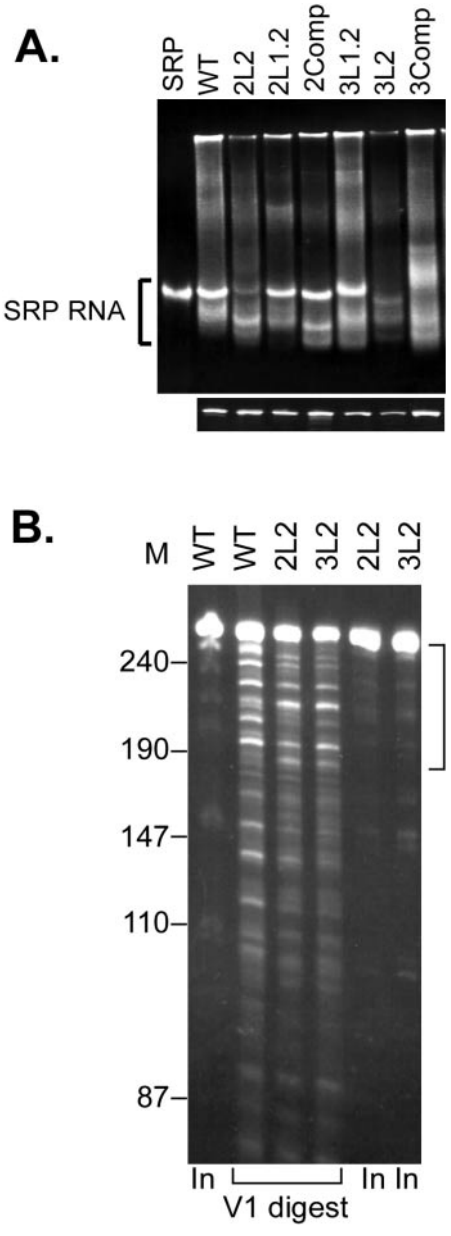

Figure 3. Analysis of wild-type and mutated synthetic SRP RNAs. (**A**) Native (upper panel) and denaturing (lower panel) 6% PAGE. Equal amounts of RNA were loaded on both gels. The RNAs were visualized by staining with Gelstar®. SRP RNA was extracted from purified canine SRP. The synthetic RNAs are labelled as shown in Table 1. (**B**) Limited V1 ribonuclease digestion experiments. The digestion products were displayed by 10% denaturing PAGE and the RNA fragments visualized with ethidium bromide staining. The bracket highlights the region that contains RNAs obtained by single cleavages in the *Alu* portion of SRP RNA. In, 50% of the RNA used in the experiments.

non-native structures most likely formed during synthesis and precipitation. Nevertheless, synthetic WT SRP RNA and RNAs with mutations in loop L1.2 (WT, 2L1.2 and 3L1.2) each have a major RNA band co-migrating with canine SRP RNA. This suggested that they might contain a large fraction of RNA with an active conformation. In contrast, 2L2 and 3L2 RNAs showed a dramatic change in their migration pattern consistent with major changes in RNA conformation.

To confirm that the different migration of 2L2 and 3L2 RNAs could be explained by conformational changes in a significant fraction of the RNAs, we used the double-strand-specific ribonuclease V1 under conditions which allow only one cleavage per RNA molecule. This allows the detection of the most sensitive sites in the RNA, some of which are known to be located in the *Alu* domain [(29); Materials and Methods]. Single cleavages within the *Alu* domain, which encompasses the 100 and 50 nt at the 5′ and 3′ ends, respectively, are predicted to produce RNAs with sizes >200 nt. It was obvious that the patterns of the major bands seen with WT and 2L2 and 3L2 RNAs were significantly different within the *Alu* domain-specific region (Figure 3B) consistent with RNA folding defects.

These results indicated that disrupting base pairing with mutations in loop L2 strongly diminished proper folding of the mutated RNAs leading to a large fraction of non-native conformations that migrate fast in native gels. Importantly, compensatory changes in loop L1.2 appeared to rescue proper folding of the RNA (2Comp RNA), suggesting a role of the tertiary structure in folding of the RNA. The 3Comp RNA failed to migrate as a defined band but instead migrated slightly slower than canine SRP RNA in a large band, as if it was in a native-like but more 'loosely' folded state.

Base pairing is important for proper folding of the RNA

To assess the folding defects in the *Alu* domain of the SRP RNA variants, we decided to set up a quantitative SRP9/14 binding assay. Based on the crystal structure of the complex, local changes in the loops are not expected to reduce the affinity of SRP9/14 for SRP RNA, since they are quite distant from the protein-binding site (Figure 1C). However, effects of the mutations on RNA folding are expected to increase the fraction of non-native RNA conformations that cannot bind SRP9/14. We used recombinant human SRP9/14 (h9/14) and biotinylated SRP RNA for complex formation and the free protein and the complex were separated by immobilized streptavidin. To ensure stoichiometric binding, the RNA–protein complexes were formed at concentrations far above the dissociation constant of the wild-type complex (50- to 100-fold), which is in the subnanomolar range (34,38). To monitor binding, *in vitro*-synthesized [^{35}S]methionine-labelled h14 protein bound to recombinant h9 was used as a tracer in the reactions. The bound fractions were analysed with SDS–PAGE and quantified by phosphorescence imaging (Materials and Methods).

We optimized the binding conditions for WT RNA in titration experiments. We monitored the protein-binding efficiency as a function of the RNA concentration (10–200 nM) while keeping the protein concentration constant at 40 nM. As expected for stoichiometric binding, there was a linear relationship between RNA concentrations and the protein-binding efficiencies (Figure 4). We found that 27% of the RNA and 62% of the protein could form a ribonucleoprotein complex. The finding that not all of the *in vitro* synthesized

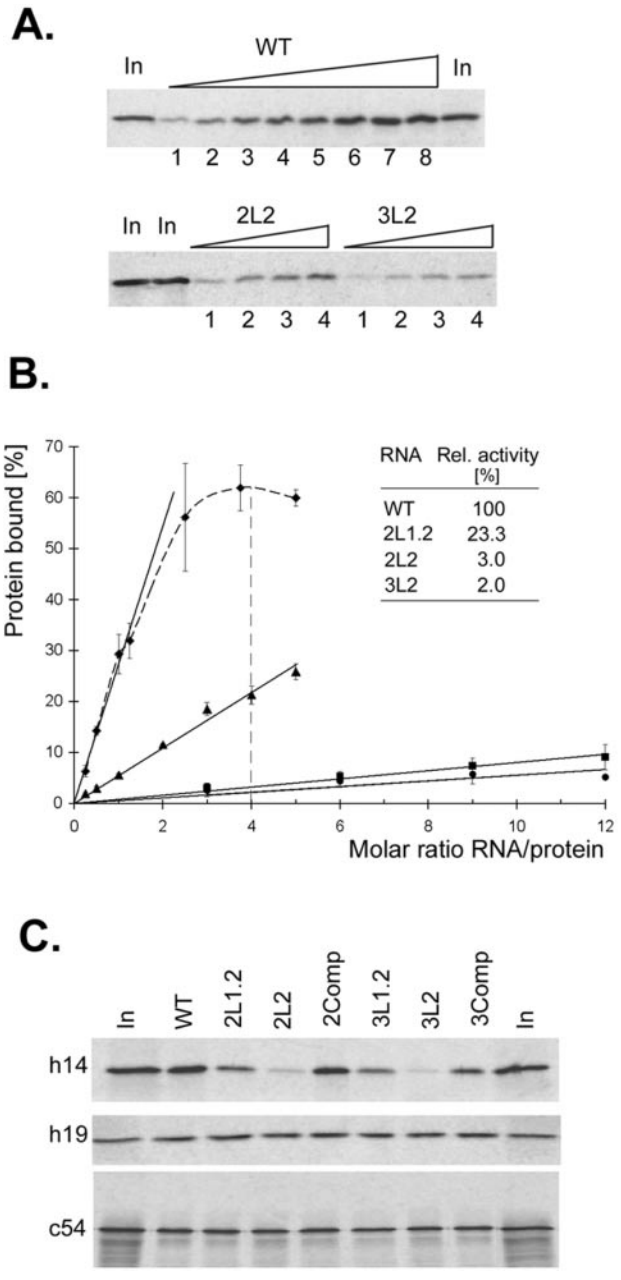

Figure 4. Binding of human SRP9/14 to mutated SRP RNAs. (**A**) Titration experiments with synthetic WT; 2L2 and 3L2 biotinylated RNAs. The binding reactions contained 40 nM h9/14 and tracer amounts of ^{35}S-labelled h14 in complex with recombinant h9. WT RNA concentrations in lanes 1–8: 10, 20, 30, 40, 50, 100, 150 and 200 nM. 2L2 and 3L2 RNA concentrations in lanes 1–4: 60, 120, 240 and 480 nM. In, 50% of total protein used in the experiment. The bound protein was displayed by SDS–PAGE followed by autoradiography. (**B**) Quantitative analysis of the titration experiments. WT (diamonds), 2L1.2 (triangles), 2L2 (squares) and 3L2 (dots) RNAs. (**C**) Protein binding with the mutated synthetic SRP RNAs. The protein and RNA concentrations were 40 and 160 nM, respectively, in the binding reactions. The binding reactions of c54 also contained 40 nM recombinant h19. The quantification of the results is shown in Table 2.

RNA was active was expected from the previous results (native gel, Figure 3). An additional fraction of the RNA might have been inactivated because of the presence of a biotinylated uridine instead of a regular uridine at critical positions in the RNA (Figure 1). In subsequent experiments we determined the relative activities of mutated RNAs as compared with WT RNA. Since the number and location of the U residues are identical in all the RNA variants analysed, biotinylation was not expected to interfere with the comparative analysis. In addition, it was not necessary to take into account the activity of the protein. Further control experiments indicated that the RNA–protein complexes were stable during the wash and that a negative control RNA gave no detectable signal (see Materials and Methods). We chose to use a 4-fold excess of RNA over the protein (dashed line in Figure 4B) and binding of WT RNA was set to 100% (Figure 4C, upper panel and Table 2).

The activities of 2L2 and 3L2 RNAs were very low as expected if a major fraction of the RNA was misfolded. The activities of RNAs with mutations in loop L1.2 (2L1.2 and 3L1.2 RNAs) was reduced ~3-fold compared with WT RNA, suggesting that these RNAs were also misfolded, albeit to a lesser extent. The fact that they could bind h9/14 to a significant extent is consistent with the presence of an SRP-RNA-specific band in the native gel. Complementary mutations in both loops (2Comp, 3Comp) restored binding, establishing a role of base pairing in RNA folding. This is surprising for 3Comp RNA, because this RNA migrates in an odd native-like manner in native gels. It might, therefore, still harbour minor conformational defects that are only partially detected by SRP9/14 binding.

To corroborate that reduced binding was explained by misfolding and not by a reduced affinity of the protein for the RNA, we repeated the titration experiment with 2L1.2, 2L2 and 3L2 RNAs (Figure 4A and B). There was a linear relationship between RNA concentration and protein binding as was expected, if a fraction of the RNA was misfolded while the affinity of the protein to the active fraction of the RNA remained the same. Hence, these results confirmed that protein binding was a valuable way to determine the folding efficiencies of mutated SRP RNAs. The activities of the RNAs were calculated from the slope of the straight lines (Figure 4B, inset). The effects of the mutations were the same as previously seen in the comparative protein-binding assays (Table 2).

We also tested whether the presence of all the other SRP proteins in the binding reactions (recombinant h19 and c54, canine SRP68/72, Materials and Methods) and re-annealing of SRP RNA might improve the binding efficiencies of the mutated RNAs. We had shown previously that the minimal *Alu* RNA that still binds h9/14 with full efficiency (SA86) could be folded *in vitro* (29). With SRP RNA, however, there were no significant improvements of the h9/14 binding capacities of the RNAs (Table 2). Even worse, we noticed that re-annealing abrogated SRP54 binding (Table 2) indicating that the S domain became misfolded.

In summary, disrupting the tertiary structure with mutations in either loop result in a negative asymmetric effect on RNA folding during its synthesis. Complementary mutations significantly rescue proper folding of the RNA. These results establish that base pairing takes place in complete SRP RNA and that it is important for the efficient assembly of the SRP *Alu* domain.

Table 2. Effects of mutations in loops L1.2 and L2 of SRP RNA on protein-binding efficiencies and on functional activities of reconstituted particles

RNAs	Protein-binding efficiencies (%)				Activities of particles (%)	
	9/14	9/14[a]	19	54	EA	T
WT	100	100	100	100	100	100
2L2	8	9	90	78	—	—
3L2	4	4	80	79	—	—
2L1.2	30	31	104	94	93	100
3L1.2	30	29	95	81	64	71
2Comp	86	85	119	96	93	125
3Comp	44	50	101	96	86	101
WT refold.	103	112	—	20	—	—
2L2 refold.	5	9	—	—	—	—
Buffer	—	—	—	—	0	23

The RNA and protein concentrations in the binding reactions were 160 and 40 nM, respectively. Binding efficiencies were normalized to WT SRP RNA, which was set to 100%. Average standard deviations for protein binding (%): 4.3 (9/14), 3.8 (19) and 4.6 (54). EA, elongation arrest activity; T, translocation efficiency. EA and T were set to 100% for WTSRP. Translocation in the absence of SRP is due to microsome-bound SRP. Average standard deviations were 7% for EA and T.

[a]9/14 binding was assayed in the presence of all other SRP proteins. C54 binding was assayed in the presence of 40 nM h19. Particles were reconstituted using a 2-fold excess of SRP RNAs together with all SRP proteins and the activities of the reconstitution reactions were assayed directly.

Protein binding to the S domain is not significantly affected by the mutations in the *Alu* domain

We repeated the comparative protein-binding experiments with human SRP19 (h19) and h19 together with canine SRP54 (c54). SRP54 binding to SRP RNA is dependent on the presence of SRP19 (39). Binding was monitored by the addition of trace amounts of [^{35}S]methionine-labelled h19 or c54 synthesized in wheat germ extract in the presence of recombinant proteins. The binding reactions were done as before at final concentrations of 40 and 160 nM of protein and RNA, respectively. In general, there was no major effect on binding of c54 and h19 to the mutated RNAs, suggesting that the S domain was capable of folding independently (Figure 4C and Table 2). However, 2L2, 3L2 and 3L1.2 RNAs had slightly reduced protein-binding activities, consistent with the presence of small fractions of completely misfolded SRP RNAs. As with h9/14 binding, the small defects in h19 and c54 binding were restored to WT levels in the RNAs with compensatory mutations, consistent with the interpretation that misfolding of the *Alu* domain interfered with S domain folding to a low extent.

Mutations do not interfere with SRP activities

To assess whether the mutated SRP RNAs were capable of conferring elongation arrest and targeting activities to SRP, it was necessary to reconstitute particles from the *in vitro*-synthesized RNAs and all SRP proteins (8,36). The reconstituted particles were then added to *in vitro* translation reactions to assay their activities. The relative inhibition of preprolactin synthesis (a secreted protein) as compared with cyclin D synthesis

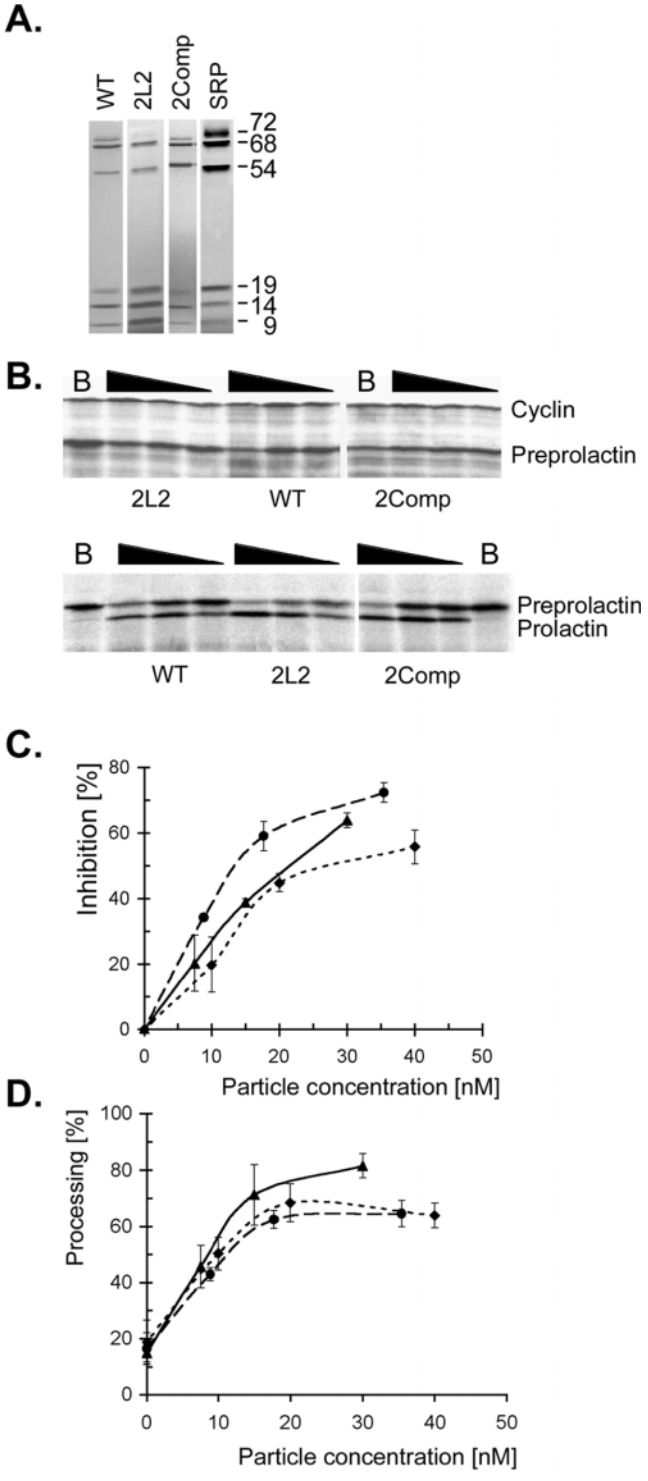

Figure 5. Elongation arrest and translocation activities of particles reconstituted with mutated SRP RNAs. (**A**) Fractions enriched in complete SRP that was reconstituted *in vitro* with all SRP proteins and WT, 2L2 and 2Comp synthetic RNAs. (**B**) Elongation arrest (upper panel) and translocation (lower panel) assays with 2, 1, 0.5 and 0 µl (B, Buffer) of the fractions shown in (A). Translocation assays contain SRP-depleted microsomes. B, buffer. (**C** and **D**) Quantification of the elongation arrest and translocation assays. The ratio of preprolactin to cyclin in the buffer sample was taken as 0% inhibition in the elongation arrest assay. In the absence of exogenous SRP, the membranes have a residual translocation activity of about 20%. Values represent the average of at least two independent experiments. WT SRP (diamonds), 2L2 SRP (triangles) and 2Comp SRP (dots).

(a cytoplasmic protein) was monitored to determine elongation arrest activities. To examine the signal recognition and targeting activities of the particles, we assayed their ability to promote translocation of preprolactin into salt-washed canine microsomes as revealed by the processing of preprolactin to prolactin.

Since 2L2 and 3L2 RNAs had only a very low ability to bind h9/14 and, therefore, to assemble into complete SRP, it was necessary to do the reconstitution reactions in the presence of excess of RNA over protein to obtain detectable amounts of SRP. Because translation of preprolactin and cyclin was severely inhibited by the addition of high levels of RNA, we enriched completely reconstituted mutant SRP by anion exchange chromatography (Materials and Methods). It is known that functional canine SRP elutes at 600 mM potassium acetate from a DEAE column (36,39). At the same time, we also reconstituted WT and 2Comp particles. The fractions containing all SRP proteins were assayed for activities (Figure 5A and B). The maximal concentrations of potentially active SRP that might be present in these fractions were estimated from the intensities of the c54 signal. The 2L2 and 2Comp fractions showed concentration-dependent elongation arrest and translocation activities comparable to the one of the WT fraction (Figure 5C and D). Hence, the mutations in 2L2 and 2Comp RNAs did not interfere with the elongation arrest and translocation activities of reconstituted particles.

Similar experiments with 3L2 RNA failed to yield detectable amounts of active SRP in the fractions eluting from the anion exchange columns, even when using higher amounts of RNA in the reconstitution reactions probably because the presence of too much RNA eventually abolishes assembly of functional SRP.

To test the other RNAs that had lower assembly defects, we assayed directly the reconstitution reactions for elongation arrest and translocation activities (Materials and Methods). The activities of particles containing mutated RNAs were normalized to the activities of fully reconstituted particles containing WT RNA (Table 2). SRPs comprising 2L1.2, 2Comp and 3Comp RNAs had elongation arrest and translocation activities comparable to WT SRP whereas 3L1.2 SRP had slightly diminished activities. The latter was most likely explained by its reduced c54 binding activity.

Five of the six mutated SRP RNAs could be assembled into fully functional particles, thereby demonstrating that the mutations had no direct impact on the elongation arrest activity.

DISCUSSION

An important step in the assembly of functional ribonucleoprotein complexes is the proper folding of the RNA subunit. Folding is not a trivial problem, especially for larger RNAs, since once trapped in non-native conformations, RNA secondary structures cannot be easily converted into native structures because of the high stability of even small helical stems. Our results underscore the primary importance of a tertiary structure for proper folding of SRP RNA and they therefore define the loop–loop base pairs as a key architectural element for the assembly of functional SRP.

Co-transcriptional folding is a vectorial process, and local secondary and tertiary structures might form as soon as the RNA exits the transcription complex [for review see (2,40)]. As yet, we can only speculate on the folding pathway of the *Alu* domain. However, the results presented highlight two important events that might control the early steps of SRP RNA folding. First, the formation of the first hairpin structure including loop L2 sequences appears to be very critical and, second, the recruitment of SRP9/14, which is required for SRP function, depends strongly on proper folding, and hence, on the tertiary structure of SRP RNA. These findings suggest a series of sequential events that might control folding of the SRP RNA *Alu* domain (Figure 6).

The first rigid element to emerge from the transcription complex is the conserved U-turn in loop L2. Together with the other loop L2 sequences and the stable G-C-rich helix H2, it might ensure efficient and the fast formation of the first hairpin (Figure 6, step 1). The next rigid element to emerge is the U-turn of the conserved protein-binding site. It will determine the orientation of the emerging strand facilitating loop–loop interactions (step 2). Base pairing between the loops (step 3) further stabilizes the central U-turn, which can now be recognized by the protein SRP9/14. At this point, SRP9/14 may act as an early checkpoint for proper folding of the RNA as it can distinguish between native and non-native conformations (step 4). In addition, it may assist proper folding of certain native-like conformations at this point or possibly already in the earlier step (steps 3 and 4). Protein binding locks the stem alignment and the base pairs into place and thereby facilitates the formation and stacking of stems H1.2 and H1.1 (step 5).

Once the *Alu* 5′ domain is properly assembled, folding and assembly of the S domain will ensue. The final step of SRP assembly is the formation of the 3′ half of the central stem (Figure 1). Based on earlier studies, formation of the central stem will allow the *Alu* 5′ domain to flip by 180° to align besides the central stem. The central stem (Figure 1, *Alu* 3′ domain) can then bind to the protein SRP9/14 (25,28). The last step might represent a final checkpoint for SRP assembly before its export to the cytoplasm.

According to this model, SRP9/14 would have a pivotal role in SRP assembly *in vivo*. It may act as a sensor of properly folded RNA and of properly assembled SRP in the assembly pathway. SRP14 has been found in nucleoli of mammalian and yeast cells (16,20) and it might, therefore, be present during synthesis of the RNA, although the transcription sites of the SRP RNA gene have not yet been identified. As yet, it is unclear whether archaeal and eubacterial organisms contain 9/14-like proteins. It is possible that the extended interactions between the loops may compensate for its absence in the early folding events.

The fact that mutations in loop L2 have a more dramatic effect on folding indicates that these mutations not only interfere with base pairing but possibly also with the formation of the crucial first hairpin structure. Based on a strictly sequential mode of events, it is difficult to understand how compensatory changes in loop L1.2 can rescue proper folding of the mutated first hairpin. However, it is possible that pairing rearrangements may be mediated by the tertiary structure. Formation of secondary structures as a function of native tertiary structures has been observed previously in folding studies (41–43). Our results also indicate that 1 bp is not sufficient to ensure proper folding. In the loop alignments, there is a strong bias for G-C base pairs and, with the exception of plants, at least three G-C pairs have been conserved in all SRP RNAs (Figure 2), consistent with the requirement of a minimal free energy for base pairing to occur.

The primary importance of the tertiary structure is its role in the assembly of functional SRP. It is conceivable that it might also play a role in the elongation arrest function. However, based on the results presented here, this function would not include sequence- or structure-specific interactions between the tertiary structure and the ribosome. This conclusion is also supported by the phylogenetic analysis, which predicts considerable changes in the specific structure of the base pairing loops between RNAs from different organisms. Yet, structures interacting directly with the ribosome are likely to be conserved. In the absence of a structure that is strikingly conserved between RNAs of all organisms, it is at this point impossible to predict whether there is a functionally decisive element in the RNA moiety. The RNA is likely to determine the position of the *Alu* domain in the elongation factor binding site (13,44) and might, therefore, put the protein SRP9/14 into the right place to exert its essential function in delaying nascent chain elongation by mammalian and yeast SRPs (8,9).

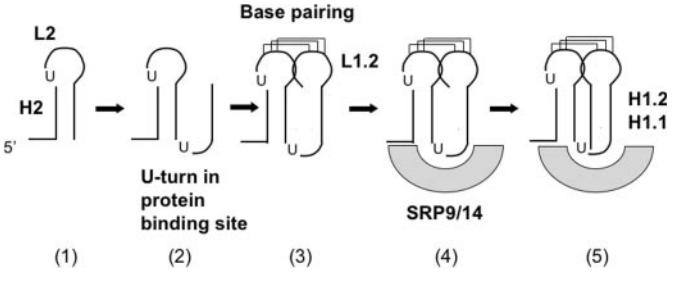

Figure 6. Model for the early steps of SRP RNA folding. Step (1) formation of the first very stable hairpin structure; step (2) the central U-turn ensures orientation of the emerging strand to allow base pairing with loop L2 [step (3)]; SRP9/14 recognizes the correctly folded central U-turn region and by binding to it stabilizes the fold [step (4)]; formation and alignment of H1.2 and H1.2 ensues [step (5)]. It is possible that the protein may bind the U-turn before base pairing occurs.

ACKNOWLEDGEMENTS

We would like to thank Dr Gilles Moreau for helpful and stimulating discussions, Dr Muriel Grange Midroit for working out the optimal conditions for biotinylation of the RNA and Monique Fornallaz, Yiwei Miao and Yuanlong Shao for technical assistance. This work was supported by grants from the Swiss National Science Foundation, the Canton of Geneva and the MEDIC Foundation. S.C. and K.S. wish to acknowledge long-term support from the Swiss Government and the European Union Framework IV TMR programme for SRPNET (FMRX-CT960035) and Framework V Quality of Life programme for MEMPROT-NET (QLK3-CT200082). Support from NIH grants R01GM26494 and the Robert A. Welch Foundation are also acknowledged (A.E.J.).

REFERENCES

1. Weeks,K.M. (1997) Protein-facilitated RNA folding. *Curr. Opin. Struct. Biol.*, **7**, 336–342.
2. Woodson,S.A. (2000) Recent insights on RNA folding mechanisms from catalytic RNA. *Cell Mol. Life Sci.*, **57**, 796–808.
3. Walter,P. and Johnson,A.E. (1994) Signal sequence recognition and protein targeting to the endoplasmic reticulum membrane. *Annu. Rev. Cell Biol.*, **10**, 87–119.
4. Johnson,A.E. and van Waes,M.A. (1999) The translocon: a dynamic gateway at the ER membrane. *Annu. Rev. Cell Dev. Biol.*, **15**, 799–842.
5. Keenan,R.J., Freymann,D.M., Stroud,R.M. and Walter,P. (2001) The signal recognition particle. *Annu. Rev. Biochem.*, **70**, 755–775.
6. Siegel,V. and Walter,P. (1985) Elongation arrest is not a prerequisite for secretory protein translocation across the microsomal membrane. *J. Cell Biol.*, **100**, 1913–1921.
7. Hauser,S., Bacher,G., Dobberstein,B. and Lutcke,H. (1995) A complex of the signal sequence binding protein and the SRP RNA promotes translocation of nascent proteins. *EMBO J.*, **14**, 5485–5493.
8. Thomas,Y., Bui,N. and Strub,K. (1997) A truncation in the 14 kDa protein of the signal recognition particle leads to tertiary structure changes in the RNA and abolishes the elongation arrest activity of the particle. *Nucleic Acids Res.*, **25**, 1920–1929.
9. Mason,N., Ciufo,L.F. and Brown,J.D. (2000) Elongation arrest is a physiologically important function of signal recognition particle. *EMBO J.*, **19**, 4164–4174.
10. Wild,K., Weichenrieder,O., Strub,K., Sinning,I. and Cusack,S. (2002) Towards the structure of the mammalian signal recognition particle. *Curr. Opin. Struct. Biol.*, **12**, 72–80.
11. Nagai,K., Oubridge,C., Kuglstatter,A., Menichelli,E., Isel,C. and Jovine,L. (2003) Structure, function and evolution of the signal recognition particle. *EMBO J.*, **22**, 3479–3485.
12. Doudna,J.A. and Batey,R.T. (2004) Structural insights into the signal recognition particle. *Annu. Rev. Biochem.*, **73**, 539–557.
13. Halic,M., Becker,T., Pool,M.R., Spahn,C.M., Grassucci,R.A., Frank,J. and Beckmann,R. (2004) Structure of the signal recognition particle interacting with the elongation-arrested ribosome. *Nature*, **427**, 808–814.
14. Politz,J.C., Lewandowski,L.B. and Pederson,T. (2002) Signal recognition particle RNA localization within the nucleolus differs from the classical sites of ribosome synthesis. *J. Cell Biol.*, **159**, 411–418.
15. Politz,J.C., Yarovoi,S., Kilroy,S.M., Gowda,K., Zwieb,C. and Pederson,T. (2000) Signal recognition particle components in the nucleolus. *Proc. Natl Acad. Sci. USA*, **97**, 55–60.
16. Andersen,J.S., Lyon,C.E., Fox,A.H., Leung,A.K., Lam,Y.W., Steen,H., Mann,M. and Lamond,A.I. (2002) Directed proteomic analysis of the human nucleolus. *Curr. Biol.*, **12**, 1–11.
17. Jacobson,M.R. and Pederson,T. (1998) Localization of signal recognition particle RNA in the nucleolus of mammalian cells. *Proc. Natl Acad. Sci. USA*, **95**, 7981–7986.
18. Alavian,C.N., Politz,J.C., Lewandowski,L.B., Powers,C.M. and Pederson,T. (2004) Nuclear export of signal recognition particle RNA in mammalian cells. *Biochem. Biophys. Res. Commun.*, **313**, 351–355.
19. Dean,K.A., von Ahsen,O., Gorlich,D. and Fried,H.M. (2001) Signal recognition particle protein 19 is imported into the nucleus by importin 8 (RanBP8) and transportin. *J. Cell Sci.*, **114**, 3479–3485.
20. Grosshans,H., Deinert,K., Hurt,E. and Simos,G. (2001) Biogenesis of the signal recognition particle (SRP) involves import of SRP proteins into the nucleolus, assembly with the SRP-RNA, and Xpo1p-mediated export. *J. Cell Biol.*, **153**, 745–762.
21. Gorodkin,J., Knudsen,B., Zwieb,C. and Samuelsson,T. (2001) SRPDB (Signal Recognition Particle Database). *Nucleic Acids Res.*, **29**, 169–170.
22. Strub,K., Moss,J. and Walter,P. (1991) Binding sites of the 9- and 14-kilodalton heterodimeric protein subunit of the signal recognition particle (SRP) are contained exclusively in the Alu domain of SRP RNA and contain a sequence motif that is conserved in evolution. *Mol. Cell. Biol.*, **11**, 3949–3959.
23. Beja,O., Ullu,E. and Michaeli,S. (1993) Identification of a tRNA-like molecule that copurifies with the 7SL RNA of *Trypanosoma brucei*. *Mol. Biochem. Parasitol.*, **57**, 223–229.
24. Liu,L., Ben-Shlomo,H., Xu,Y.X., Stern,M.Z., Goncharov,I., Zhang,Y. and Michaeli,S. (2003) The trypanosomatid signal recognition particle consists of two RNA molecules, a 7SL RNA homologue and a novel tRNA-like molecule. *J. Biol. Chem.*, **278**, 18271–18280.
25. Weichenrieder,O., Wild,K., Strub,K. and Cusack,S. (2000) Structure and assembly of the Alu domain of the mammalian signal recognition particle. *Nature*, **408**, 167–173.
26. Larsen,N. and Zwieb,C. (1991) SRP-RNA sequence alignment and secondary structure. *Nucleic Acids Res.*, **19**, 209–215.
27. Zwieb,C., Muller,F. and Larsen,N. (1996) Comparative analysis of tertiary structure elements in signal recognition particle RNA. *Fold. Des*, **1**, 315–324.
28. Weichenrieder,O., Stehlin,C., Kapp,U., Birse,D.E., Timmins,P.A., Strub,K. and Cusack,S. (2001) Hierarchical assembly of the Alu domain of the mammalian signal recognition particle. *RNA*, **7**, 731–740.
29. Weichenrieder,O., Kapp,U., Cusack,S. and Strub,K. (1997) Identification of a minimal Alu RNA folding domain that specifically binds SRP9/14. *RNA*, **3**, 1262–1274.
30. Arnaud,N., Cheynet,V., Oriol,G., Mandrand,B. and Mallet,F. (1997) Construction and expression of a modular gene encoding bacteriophage T7 RNA polymerase. *Gene*, **199**, 149–156.
31. Lingelbach,K., Zwieb,C., Webb,J.R., Marshallsay,C., Hoben,P.J., Walter,P. and Dobberstein,B. (1988) Isolation and characterization of a cDNA clone encoding the 19 kDa protein of signal recognition particle (SRP): expression and binding to 7SL RNA. *Nucleic Acids Res.*, **16**, 9431–9442.
32. Romisch,K., Webb,J., Lingelbach,K., Gausepohl,H. and Dobberstein,B. (1990) The 54-kD protein of signal recognition particle contains a methionine-rich RNA binding domain. *J. Cell Biol.*, **111**, 1793–1802.
33. Bovia,F., Fornallaz,M., Leffers,H. and Strub,K. (1995) The SRP9/14 subunit of the signal recognition particle (SRP) is present in more than 20-fold excess over SRP in primate cells and exists primarily free but also in complex with small cytoplasmic Alu RNAs. *Mol. Biol. Cell*, **6**, 471–484.
34. Bovia,F., Wolff,N., Ryser,S. and Strub,K. (1997) The SRP9/14 subunit of the human signal recognition particle binds to a variety of Alu-like RNAs and with higher affinity than its mouse homolog. *Nucleic Acids Res.*, **25**, 318–326.
35. Studier,F.W., Rosenberg,A.H., Dunn,J.J. and Dubendorff,J.W. (1990) Use of T7 RNA polymerase to direct expression of cloned genes. *Methods Enzymol.*, **185**, 60–89.
36. Chang,D.Y., Newitt,J.A., Hsu,K., Bernstein,H.D. and Maraia,R.J. (1997) A highly conserved nucleotide in the Alu domain of SRP RNA mediates translation arrest through high affinity binding to SRP9/14. *Nucleic Acids Res.*, **25**, 1117–1122.
37. Su,L., Chen,L., Egli,M., Berger,J.M. and Rich,A. (1999) Minor groove RNA triplex in the crystal structure of a ribosomal frameshifting viral pseudoknot. *Nature Struct. Biol.*, **6**, 285–292.
38. Janiak,F., Walter,P. and Johnson,A.E. (1992) Fluorescence-detected assembly of the signal recognition particle: binding of the two SRP protein heterodimers to SRP RNA is noncooperative. *Biochemistry*, **31**, 5830–5840.
39. Walter,P. and Blobel,G. (1983) Disassembly and reconstitution of the signal recognition particle. *Cell*, **34**, 525–533.
40. Schroeder,R., Grossberger,R., Pichler,A. and Waldsich,C. (2002) RNA folding *in vivo*. *Curr. Opin. Struct. Biol.*, **12**, 296–300.
41. Wu,M. and Tinoco,I.,Jr (1998) RNA folding causes secondary structure rearrangement. *Proc. Natl Acad. Sci. USA*, **95**, 11555–11560.
42. Gluick,T.C. and Draper,D.E. (1994) Thermodynamics of folding a pseudoknotted mRNA fragment. *J. Mol. Biol.*, **241**, 246–262.
43. Silverman,S.K., Zheng,M., Wu,M., Tinoco,I.,Jr and Cech,T.R. (1999) Quantifying the energetic interplay of RNA tertiary and secondary structure interactions. *RNA*, **5**, 1665–1674.
44. Terzi,L., Pool,M.R., Dobberstein,B. and Strub,K. (2004) Signal recognition particle Alu domain occupies a defined site at the ribosomal subunit interface upon signal sequence recognition. *Biochemistry*, **43**, 107–117.